Nonlinear Processes
in Geophysics

Modelling and simulation of waves in three-layer porous media

S. R. Pudjaprasetya

Mathematics Department, Institut Teknologi Bandung, Jalan Ganesha 10, Bandung, 40132, Indonesia

Correspondence to: S. R. Pudjaprasetya (sr_pudjap@math.itb.ac.id)

Abstract. The propagation of gravity waves in an emerged three-layer porous medium is considered in this paper. Based on the assumption that the flow can be described by Darcy's Law, an asymptotic theory is developed for small-amplitude long waves. This leads to a weakly nonlinear Boussinesq-type diffusion equation for the wave height, with coefficients dependent on the conductivities and depths of each layer. In the limit of equal conductivities of all layers, the equation reduces to the single-layer result recorded in the literature. The model equations are numerically integrated in the case of an incident monochromatic wave hitting the layers. The results exhibit dissipation and also a downstream net height rise at infinity. Wave transmission coefficient in three-layer porous media with conductivity of mangrove is discussed. Numerically, propagation of an initial solitary wave through a porous medium shows the emergence of wave reflection and transmission that both evolve as permanent waves. Additionally we examine the impact of a solitary gravity wave on a porous medium breakwater.

1 Introduction

As reported in Dahdouh-Guebas (2006) and Kathiresan and Rajendran (2006), mangrove forests along coastal areas provide shelter against storms and floods, as well as tsunami. Mangrove belts can absorb wave energy and reduce wave amplitude and velocity. The amount of wave amplitude reduction in mangroves depends on factors such as water depth, coastal profile, and also mangrove species and mangrove thickness. Due to the complexity of the problems, research on mangrove protection mostly relies on field measurement data from certain areas. For instance, Teh et al. (2009) conducted a numerical and experimental study of tsunami mitigation by mangroves (*Avicennia officinalis*) on the coast of Penang, Malaysia. Liu et al. (2003) studied flow resistance of mangrove trees using a depth-averaged hydrodynamic numerical model. The model and the vegetative parameter were tested using on-site mangrove data (*Kandelia* sp.) along Keelung River, Taiwan. Masda et al. (1997) reported on the experimental study of mangroves (*Kandelia* sp.) as a coastal protection in the Tong King delta, Vietnam.

Motivated by the protective function of mangrove in mitigating high waves, here we develop a study of gravity waves in a three-layer porous medium. The three layers here are leaves, trunks, and roots layers of mangrove forest. Wave interaction with non-uniform mangrove has been considered in the following literature. Vo-Luong and Massel (2008) study wave energy dissipation in a three-layer mangrove above arbitrary depth. They use velocity potential formulations with dissipation to develop a predictive model for random waves in a non-uniform forest in water of changing depth. Massel et al. (1999) study wave attenuation in mangrove forests consisting of roots and trunks.

Generally, studying wave propagation through a porous structure has many practical applications in coastal and ocean engineering. As a breakwater, porous structures reduce the amplitude of waves propagating into the structure. Studies in this area are quite extensive; here we mention only a few of them. Sollitt and Cross (1972), Madsen (1974), and Sulisz (1985) developed a linear wave model for progressive waves in a finite thickness of breakwater, and studied wave reflection and transmission far away from the porous structures. Experimental and numerical studies of wave interaction with a finite thickness of porous structure are discussed for instance in Fernando et.al. (2008), van Gent (1995), Lynett et.al. (2000), Lin and Karunarathna (2007), Liu et al. (1999), and Scarlatos and Singh (1987). These authors use the modified shallow water fluid flow equations to take into account frictional dissipation. Other authors, Chwang and Chan (1998), and Liu and Wen (1997), use porous media flow equations as described by Darcy's Law to describe flow through the structures. Since for thick groves, viscous effects dominate inertial effects, for our study here we adopt Darcy's

assumption, and we develop an asymptotic model for gravity waves in a rigid isotropic three-layer porous structure.

The organization of this paper is as follows. The governing equations are presented in Sect. 2. In Sect. 3 asymptotic methods are used to derive a simpler set of equations; the wave height is shown to satisfy a Boussinesq equation. It is a diffusion equation with higher-order nonlinear and dispersion terms. In Sect. 4 a predictor–corrector finite-difference scheme is used to simulate the movement of a monochromatic wave through the medium. Simulation shows amplitude reduction of waves in three-layer porous media. Numerical simulations clearly display the nonlinear effect: the rising of water levels at the right ends of rather long porous media. In Sect. 5 we use typical hydraulic conductivity of mangrove to calculate the wave transmission coefficient for a porous belt with certain length. In Sect. 6 we show that the newly derived three-layer Boussinesq model can be combined with the Boussinesq equation for free water to simulate a solitary wave passing through a porous medium, in which the predictor–corrector scheme follows through. Conclusions are given in Sect. 7.

2 Governing equations for flow in three-layer porous media

In this section, we formulate the governing equations for free-surface flow in a three-layer porous medium over an infinitely long horizontal axis. Let $\bar{\eta}(\bar{x}, \bar{t})$ denote the free surface elevation measured from the undisturbed water level; see Fig. 1. The porous medium consists of three layers: an upper, middle, and lower layer with thicknesses $\bar{h}_1$, $\bar{h}_2 - \bar{h}_1$, and $\bar{h}_3 - \bar{h}_2$, respectively, denoted as

$$\bar{\Omega}_1 = \left\{ (\bar{x}, \bar{z}) | -\bar{h}_1 \leq \bar{z} \leq \bar{\eta}(\bar{x}, \bar{t}), \bar{x} \in \mathbb{R} \right\}, \tag{1}$$

$$\bar{\Omega}_2 = \left\{ (\bar{x}, \bar{z}) | -\bar{h}_2 \leq \bar{z} \leq -\bar{h}_1, \bar{x} \in \mathbb{R} \right\}, \tag{2}$$

$$\bar{\Omega}_3 = \left\{ (\bar{x}, \bar{z}) | -\bar{h}_3 \leq \bar{z} \leq -\bar{h}_2, \bar{x} \in \mathbb{R} \right\}. \tag{3}$$

We assume that each layer $\bar{\Omega}_i$ for $i = 1, 2, 3$ is a rigid isotropic porous medium containing an ideal fluid of depth $\bar{h}_3(\bar{x})$.

Inside the porous medium we employ Darcy's law:

$$\boldsymbol{u}_i = -K_i \nabla \bar{\Phi}_i, \quad \text{where} \quad \bar{\Phi}_i = \frac{P}{\rho g} + \bar{z}, \tag{4}$$

with K_i hydraulic conductivity for each layer $i = 1, 2, 3$, with dimension m/sec. In each of the three layers, $\bar{\Omega}_i$ mass conservation requires

$$\nabla^2 \bar{\Phi}_i = 0, \quad \text{in} \quad \bar{\Omega}_i, \quad \text{for} \quad i = 1, 2, 3. \tag{5}$$

Along the free surface, the pressure P is constant and can be taken as zero; we then obtain a boundary condition

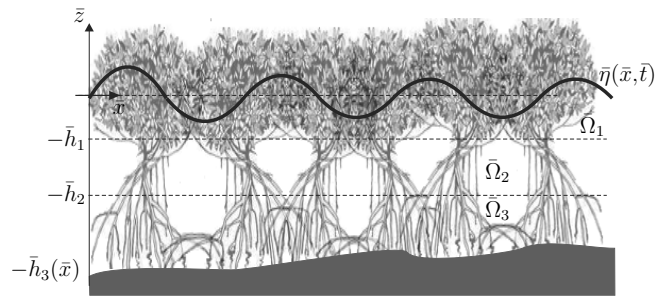$$\bar{\Phi}_1 = \bar{\eta}, \quad \text{on} \quad \bar{z} = \bar{\eta}. \tag{6}$$

Fig. 1. Schematic diagram of the emerged three-layer porous domain.

Along the two interfaces $\bar{z} = -\bar{h}_i$ the following boundary conditions hold:

$$\bar{\Phi}_i = \bar{\Phi}_{i+1} \quad \text{on} \quad \bar{z} = -\bar{h}_i \text{ for } i = 1, 2, \tag{7}$$

$$K_i \bar{\Phi}_{i\bar{z}} = K_{i+1} \bar{\Phi}_{i+1\bar{z}} \quad \text{on} \quad \bar{z} = -\bar{h}_i \text{ for } i = 1, 2. \tag{8}$$

Equation (7) comes from continuity of the pressure P, while Eq. (8) comes from the assumption that fluid influx and outflux across the interface are the same. The kinematic boundary condition along the surface is

$$\bar{\eta}_{\bar{t}} - K_1 \bar{\Phi}_{1\bar{x}} \bar{\eta}_{\bar{x}} + K_1 \bar{\Phi}_{1\bar{z}} = 0 \quad \text{on} \quad \bar{z} = \bar{\eta}. \tag{9}$$

Along the impermeable bottom $\bar{z} = -\bar{h}_3(\bar{x})$, the normal flux vanishes:

$$\bar{\Phi}_{3\bar{z}} = 0 \quad \text{on} \quad \bar{z} = -\bar{h}_3(\bar{x}). \tag{10}$$

We summarize: the governing equations for ideal fluid flow in the three-layer porous media are Eqs. (5–10).

3 Asymptotic expansion method leading to Boussinesq equation

Assuming small amplitude long wavelength, we look for asymptotic solutions $\bar{\Phi}_i$ for $i = 1, 2, 3$ of the governing Eqs. (6–10). Let L be typical length of the porous medium, $\bar{h}_3$ the fluid depth, and a typical free surface displacement. Introduce the following non-dimensional variables, written without bars as follows:

$$\bar{\eta} = a\eta, \quad \bar{z} = \bar{h}_3 z, \quad \bar{x} = Lx, \quad \bar{t} = \frac{L^2}{K_1 \bar{h}_3} t,$$

$$\bar{h}_i = \bar{h}_3 h_i, \quad \bar{\Phi}_i = a\Phi_i, \quad \text{for } i = 1, 2, 3. \tag{11}$$

Note that conductivity K_1 is scaled in the non-dimensional time variable t, and also that $h_3 \equiv \bar{h}_3 / \bar{h}_3 = 1$. Further, we denote two small parameters

$$\varepsilon = \frac{a}{\bar{h}_3}, \quad \mu^2 = \left(\frac{\bar{h}_3}{L} \right)^2. \tag{12}$$

Under the same assumption, Liu and Wen (1997) implement the asymptotic expansion method for the case of a single

layer. In this section we extend this approach for the case of three-layer porous media. Compared to this approach, our approach is more direct. Rewriting the governing Eqs. (6–10) in non-dimensional variables, equations for the first layer are

$$\mu^2 \Phi_{1xx} + \Phi_{1zz} = 0 \quad \text{in} \quad \Omega_1 \tag{13}$$

$$\Phi_1 = \eta \quad \text{on} \quad z = \varepsilon\eta \tag{14}$$

$$\mu^2 (\eta_t - \varepsilon\Phi_{1x}\eta_x) + \Phi_{1z} = 0 \quad \text{on} \quad z = \varepsilon\eta. \tag{15}$$

The equation for the second layer is

$$\mu^2 \Phi_{2xx} + \Phi_{2zz} = 0 \quad \text{in} \quad \Omega_2. \tag{16}$$

The equations for the third layer are

$$\mu^2 \Phi_{3xx} + \Phi_{3zz} = 0 \quad \text{in} \quad \Omega_3 \tag{17}$$

$$\Phi_{3z} = 0 \quad \text{on} \quad z = -h_3, \tag{18}$$

The matching conditions along the two interfaces $z = -h_i$ are

$$\Phi_i = \Phi_{i+1} \quad \text{on} \quad z = -h_i \text{ for } i = 1, 2, \tag{19}$$

$$K_i \Phi_{iz} = K_{i+1} \Phi_{i+1z} \quad \text{on} \quad z = -h_i \text{ for } i = 1, 2. \tag{20}$$

Further, we restrict to Boussinesq approximation, in which $\mathcal{O}(\varepsilon) = \mathcal{O}(\mu^2)$, and look for a solution in the form of the series

$$\Phi_i(x, z, t) = \Phi_{i0} + \mu^2 \Phi_{i1} + \mu^2 \Phi_{i2} + \cdots, \quad \text{for } i = 1, 2, 3.$$

We implement the asymptotic expansion method in the normalized governing Eqs. (13) and (20), by solving the corresponding equations layer by layer, starting from the first $\mathcal{O}(1)$ terms, to higher order $\mathcal{O}(\mu^2)$ terms, and further to $\mathcal{O}(\mu^4)$ terms. Hence, an explicit approximate expression of Φ_{i1} for $i = 1, 2, 3$ can then be obtained; see Eqs. (A5), (A7), and (A10) in Appendix A, respectively. Substituting the approximate potentials into the interface condition (20) along $z = -h_2$ yields the following equation of Boussinesq type:

$$\eta_t - \mu^2 A \eta_{xxt} = (\eta_x (B + \varepsilon R_{31} \eta))_x, \tag{21}$$

with coefficients A and B dependent on the conductivity and thickness of each layer, or explicitly

$$B = h_1 + R_{21}(h_2 - h_1) + R_{31}(h_3 - h_2), \tag{22}$$

with $R_{ij} = K_i / K_j$ for $i, j = 1, 2, 3$.

$$A = \frac{1}{2}(h_2 - h_1)^2 + \frac{1}{2}h_1^2 - \frac{1}{B}\left(\frac{1}{6}h_1^3 + \frac{1}{2}h_1(h_2 - h_1)^2\right)$$

$$+ R_{21}\left\{h_1(h_2 - h_1) - \frac{1}{B}\left(\frac{1}{6}(h_2 - h_1)^3 + \frac{1}{2}h_1^2(h_2 - h_1)\right)\right\}$$

$$+ R_{31}\left\{h_1(h_3 - h_2) - \frac{1}{B}\left(\frac{1}{6}(h_3 - h_2)^3 + \frac{1}{2}\left[(h_2 - h_1)^2\right.\right.\right.$$

$$\left.\left.\left. -(h_3 - h_2)^2 + h_1^2\right](h_3 - h_2)\right)\right\}$$

$$+ R_{32}\left\{(h_2 - h_1)^2 - \frac{1}{B}h_1(h_2 - h_1)^2\right\}. \tag{23}$$

The detail derivation of Eq. (21) is given in Appendix A. The Boussinesq equation above, written in normalized variables, is a model for gravity waves in an emerged three-layer porous medium; it is a diffusive equation with higher-order nonlinearity and dispersion.

The horizontal flux of fluid in the three-layer porous media is given by

$$Q(x, t) \equiv -\int_{-h_1}^{\varepsilon\eta} \Phi_{1x} dz - R_{21} \int_{-h_2}^{-h_1} \Phi_{2x} dz - R_{31} \int_{-h_3}^{-h_2} \Phi_{3x} dz. \tag{24}$$

Since the potential Φ_i for each layer was already approximated, substituting $(\Phi_i)_x$, for $i = 1, 2, 3$ yields the following relation:

$$Q - \mu^2 C Q_{xx} = -(B + \varepsilon\eta)\eta_x, \tag{25}$$

with

$$C = \frac{1}{3B}h_1^3 - \frac{R_{21}}{B}\left(\frac{1}{6}(h_2 - h_1)^3 + \frac{1}{2}h_1^2(h_2 - h_1)\right)$$

$$+ \frac{R_{31}}{B}\left(\frac{1}{3}(h_3 - h_2)^3 - \frac{1}{2}h_2(h_2 - h_1)(h_3 - h_2)\right). \tag{26}$$

Hence, Eqs. (21) and (25) are Boussinesq models for gravity waves in three-layer porous media. It is interesting to note that the flux and surface displacement equations are only weakly coupled; after solving for the displacement using Eq. (21), the flux can be obtained using Eq. (25). This is different from the fully coupled equations that arise from the corresponding shallow water (free) flow problem. The reason for this can be explained as follows. Under Darcy's assumption, we get boundary condition (14) which gives us the first-order term $\Phi_{10}(x, t) = \eta(x, t)$. From the asymptotic expansion framework, the first-order terms of Eq. (19) result in $\Phi_{20}(x, t) = \Phi_{10}(x, t) = \eta(x, t)$, and further $\Phi_{30}(x, t) = \Phi_{20}(x, t) = \eta(x, t)$. Since the first-order term of all potential Φ_i, $i = 1, 2, 3$ is just $\eta(x, t)$, the leading-order term in the continuity equation $\eta_t + Q_x = 0$ is just a diffusion equation with a diffusive term proportional to η_{xx}.

Next, we take a zero test where the three layers reduce to one layer. For this purpose we take $h_1 = h_2 = h_3$ for which $K_3 = K_2 = K_1$, then the dispersion coefficient and diffusion coefficients become $A = \frac{1}{3}h_3^2$ and $B = h_3$ respectively, and further $C = \frac{1}{3}h_3^2$. Hence, Eqs. (21) and (25) reduce to

$$\eta_t - \mu^2 \frac{1}{3}h_3^2 \eta_{xxt} = (\eta_x(h_3 + \varepsilon\eta))_x \tag{27}$$

$$Q - \frac{1}{3}h_3^2 Q_{xx} = -(h_3 + \varepsilon\eta)\eta_x, \tag{28}$$

respectively. The set of Eqs. (27) and (28) is equivalent to the Boussinesq equations for flow in one-layer porous media as derived in Liu and Wen (1997) using a slightly different asymptotic expansion.

4 Wave damping in porous media

Comparing Eqs. (21) and (25) for the three-layer model with the corresponding results (27, 28) for the single layer, it can be seen that waves propagating into three layers behave like those propagating into a single layer. Note that the model developed in this paper is based on the assumption that the waves are long compared to depth. For waves of wavelength comparable with the depth (or shorter), the velocity profile would vary significantly with depth, and the single- and three-layer models would likely produce different results.

For small amplitude displacements η, Eq. (27) can be approximated by the linear diffusion equation

$$\eta_t - \mu^2 A \eta_{xxt} = B \eta_{xx},$$

with wave-like solutions of the form $\exp i(kx - \omega t)$. Substituting this yields $i\omega + i\omega\mu^2 A k^2 = B k^2$ or

$$k = \sqrt{\frac{i\omega}{B - i\omega\mu^2 A}} = (1+i)\sqrt{\frac{\omega}{2B}}\left(1 + \frac{i\omega A}{B}\mu^2\right.$$
$$\left. - \frac{\omega^2 A^2}{B^2}\mu^4 + \cdots\right)^{1/2} \approx (1+i)\sqrt{\frac{\omega}{2B}}.$$

The relation above means that waves of frequency ω propagating into the system decay over a distance on the order of a wavelength $\simeq 1/k$. The penetration length is strongly dependent on wave frequency ω, which is approximately $\sqrt{2B/\omega}$.

Numerical solutions to Eq. (21) are obtained using the predictor–corrector MacCormack method. The method has second-order accuracy $\mathcal{O}(\triangle x^2, \triangle t^2)$, with $\triangle x$ and $\triangle t$ the partition length of spatial and time variables, respectively. Since there is a combine derivative in term η_{xxt}, we first rewrite Eq. (21) as

$$\Psi_t = \{\eta_x (B + \varepsilon R_{31}\eta)\}_x, \quad \text{with} \quad \Psi = \eta - \mu^2 A \eta_{xx}.$$

The first step in the MacCormack method is the predictor

$$\overline{\Psi_j^{n+1}} = \Psi_j^n + \frac{\triangle t}{\triangle x^2}\left\{\varepsilon R_{31}(\eta_{j+1}^n - \eta_j^n)^2\right.$$
$$\left. + \left(B + \varepsilon R_{31}\eta_j^n\right)(\eta_{j+1}^n - 2\eta_j^n + \eta_{j-1}^n)\right\}. \quad (29)$$

Along the left or right boundary, centre difference is replaced with one-sided difference. The overline indicates predicted values. When the predicted values $\overline{\Psi_j^{n+1}}$ for $j = 1, \cdots, Nx$ are known, the predicted values $\overline{\eta_j^{n+1}}$ for $j = 1, \cdots, Nx$ can be obtained by solving the linear relation $\mathbf{D}\eta = \Psi$, with

$$\mathbf{D}_{Nx \times Nx} = \mathbf{I}_{Nx \times Nx} - \mu^2 \frac{A}{\triangle x^2}\begin{pmatrix} 0 & 0 & 0 & \cdots & 0 \\ 1 & -2 & 1 & \cdots & 0 \\ \vdots & \ddots & \ddots & \ddots & \vdots \\ 0 & \cdots & 1 & -2 & 1 \\ 0 & \cdots & 1 & -2 & 1 \end{pmatrix}. \quad (30)$$
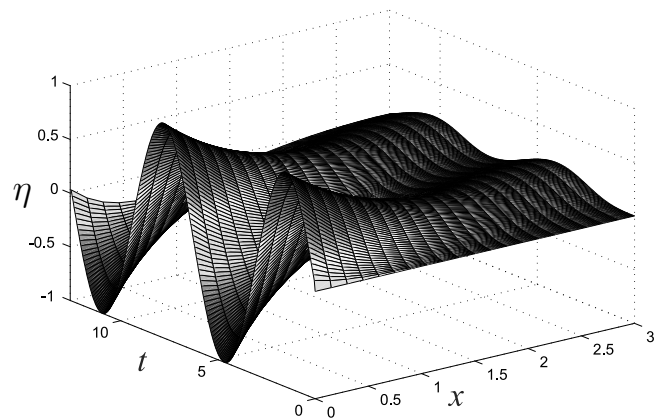

Fig. 2. A periodic tidal wave in a porous medium as the result of Eq. (21) with a significant wave reduction.

This matrix is diagonally dominant for small values of μ^2, hence it is invertible. Correction for $\overline{\Psi_j^{n+1}}$, denoted as Ψ_j^{n+1}, is calculated using the average of old values at time t_n and predicted values at time t_{n+1}, as follows:

$$\Psi_j^{n+1} = \Psi_j^n + \frac{\triangle t}{2\triangle x^2}\left\{\varepsilon R_{31}\left(\eta_{j+1}^n - \eta_j^n\right)^2 + \varepsilon R_{31}\left(\overline{\eta_{j-1}^{n+1}} - \overline{\eta_j^{n+1}}\right)^2\right.$$
$$+ \left(B + \varepsilon R_{31}\eta_j^n\right)\left(\eta_{j+1}^n - 2\eta_j^n + \eta_{j-1}^n\right)$$
$$\left. + \left(B + \varepsilon R_{31}\overline{\eta_j^{n+1}}\right)\left(\overline{\eta_{j+1}^{n+1}} - 2\overline{\eta_j^{n+1}} + \overline{\eta_{j-1}^{n+1}}\right)\right\}. \quad (31)$$

Having Ψ_j^{n+1} for $j = 1, \cdots, Nx$, we can directly compute η_j^{n+1} for the new time step, using $\eta = \mathbf{D}^{-1}\Psi$.

The above procedure is then used to simulate wave evolution in a three-layer porous medium. Initially, we have a still water level $\eta(x, 0) = 0$, then we impose a monochromatic wave influx from the left: $\eta(0, t) = \sin(t)$ or $\eta_1^n = \sin(t_n)$. Along the right boundary, we implement a transparent boundary, simply by $\eta_{Nx}^{n+1} = \eta_{Nx-1}^n$. For computations we take $\varepsilon = \mu^2 = 0.3$, and $\triangle x = \triangle t = 0.02$. We take a three-layer porous model of the same thickness, with conductivity $K_1 = 0.5$, $K_2 = 0.47$, and $K_3 = 0.5$. The surface profile reduced in the porous media is depicted in Fig. 2.

From the same computation we plot waves entering the porous medium in four different scaled frequencies: $\omega t = 0$, $\pi/2$, π, $3\pi/2$; see Fig. 3. Apart from wave reduction, we clearly observe the increase of mean water level in the far right end of the porous medium. This nonlinear phenomenon is derived in Liu and Wen (1997) as the analytical asymptotic solution of the single-layer Boussinesq model (27), in which $\eta \to \frac{\varepsilon R_{31}}{4h_3}$ for $x \to \infty$. This well-known but surprising result was observed by Nielsen (1990) in the field.
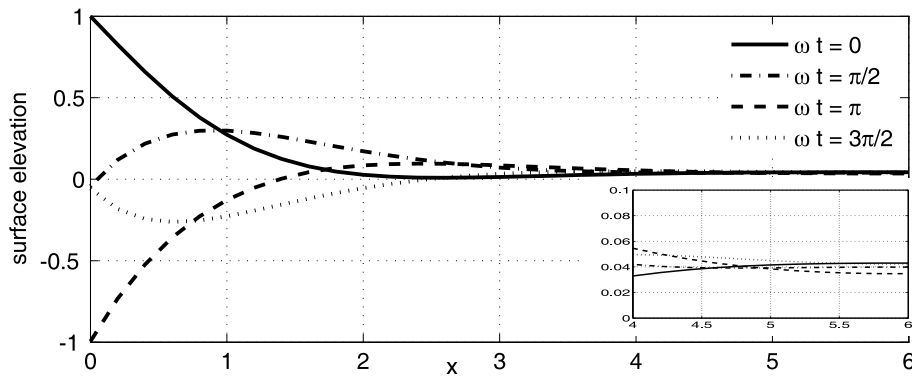
Fig. 3. Monochromatic waves enter the porous medium with four different scaled frequencies: $\omega t = 0$, $\omega t = \pi/2$, $\omega t = \pi$, $\omega t = 3\pi/2$, computed using $\varepsilon = \mu^2 = 0.3$. All four cases show the rising of mean water level as $x \to \infty$.

5 Discussion of possible application to a mangrove belt

Consider a mangrove belt as a three-layer porous medium with upper, middle and lower layers corresponding to leaves, trunks and roots of mangrove. We propose an approximate model for wave evolution in mangrove as Eq. (21). As a wave breaker, our main concern is the amount of wave energy absorbed by the breakwater. Since wave energy is proportional to the square of wave amplitude, we concern ourselves with the amount of amplitude reduction in a porous belt. Wave transmission coefficient K_T is a quantity defined as a ratio between transmitted wave and incident wave amplitudes. If the surface profile in a mangrove belt as a solution of Eq. (21) is known, then the K_T curve is just the normalized displacement of wave entering the porous medium with zero phase.

An experimental study in Susilo and Ridd (2005) reported hydraulic conductivity for mangrove (*Rhizophora* sp.) as about $10 \, \mathrm{m \, day^{-1}}$ or approximately $0.01 \, \mathrm{cm \, s^{-1}}$. Here, we solve Eq. (21) for three-layer mangrove of equal thickness, with conductivity $K_1 = 0.01 \, \mathrm{cm \, s^{-1}}$, $K_2 = 0.03 \, \mathrm{cm \, s^{-1}}$, $K_3 = 0.02 \, \mathrm{cm \, s^{-1}}$, and $\varepsilon = \mu^2 = 0.3$. We impose a monochromatic wave with period $10 \, \mathrm{s}$, or frequency $\omega = 2\pi/10 \, \mathrm{rad \, s^{-1}}$. The resulting wave transmission coefficient is given in Fig. 4. Note that the curve is plotted with respect to the physical coordinate $\bar{x} = Lx = (\bar{h}_3/\sqrt{\varepsilon})x$. In physical dimension, a point P in Fig. 4 means the following. For water depth $\bar{h}_3$ and the incident wave amplitude a that satisfies $a/\bar{h}_3 = \varepsilon = 0.3$, after passing a porous medium with length $\bar{x} = 102.2 \, \mathrm{cm}$, the wave transmission coefficient is 0.8374, which corresponds to an amplitude reduction of $\approx 16\,\%$.

For a mangrove forest with certain hydraulic conductivity, the wave transmission curve K_T clearly depends on the choice of $\varepsilon (= \mu^2)$, and on wave frequency ω. Further, we perform calculations using mangrove conductivity as above, using $\varepsilon = 0.2 - 0.6$ for several wave frequencies, and the results are given in Table 1. For mild wind waves with typical frequency $2\pi/6 \, \mathrm{rad \, s^{-1}}$, a porous belt length $100 \, \mathrm{cm}$ gives
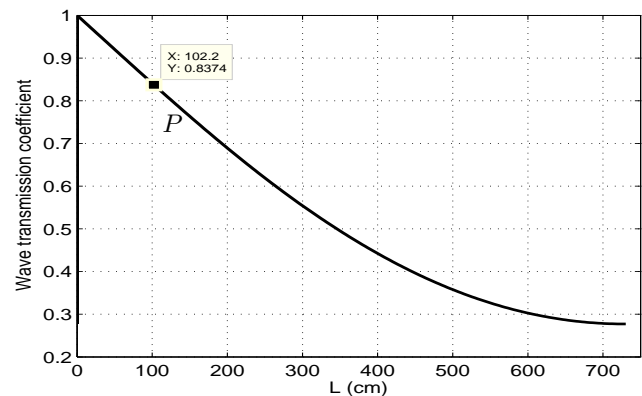

Fig. 4. Wave transmission coefficient curve from numerical computation using $\varepsilon = \mu^2 = 0.3$.

Table 1. Wave transmission coefficient calculated using conductivity $K_1 = 0.01 \, \mathrm{cm \, s^{-1}}$, $K_2 = 0.03 \, \mathrm{cm \, s^{-1}}$, and $K_3 = 0.02 \, \mathrm{cm \, s^{-1}}$ for $\varepsilon = \mu^2 = 0.2 - 0.6$.

Wave freq.	Length of mangrove belt		
($\mathrm{rad \, s^{-1}}$)	100 cm	200 cm	300 cm
$2\pi/16$ (swell)	0.86–0.90	0.73–0.81	0.62–0.72
$2\pi/10$	0.80–0.86	0.62–0.74	0.46–0.62
$2\pi/6$ (mild wind)	0.74–0.82	0.50–0.65	0.32–0.50

wave transmission coefficient 0.74–0.82. We note that the recommendation table above holds for Boussinesq waves, i.e. small-amplitude long waves, and the water depth is assumed to be constant. Moreover, reflection from the beach has been neglected.

6 Reflection of a solitary wave

In a coastal engineering context it is important to determine how much of the energy of an incoming "soliton" is absorbed by a breakwater, here the three-layer porous media.

With this in mind, we examine the impact of a soliton propagating across the ocean (depth h_3) on a finite-length porous medium of the above type. The soliton is assumed to impact normally on the medium. Of particular interest is the dependence of the transmission coefficient K_T on the length L of the porous medium with certain conductivities. The impacting wave is assumed to be long and of small amplitude such that the standard Boussinesq approximating equations

$$\bar{h}_3 \bar{\eta}_{\bar{t}} = -\left((\bar{h}_3 + \bar{\eta})\bar{q}\right)_{\bar{x}} \tag{32}$$

$$\bar{q}_{\bar{t}} - \frac{1}{3}\bar{h}_3^2 \bar{q}_{\bar{x}\bar{x}\bar{t}} = -\frac{1}{\bar{h}_3}\bar{q}\bar{q}_{\bar{x}} - g\bar{h}_3\bar{\eta}_{\bar{x}}. \tag{33}$$

are used in the free-water zone; see Whitham (1973). These equations are governing equations for bi-directional gravity waves written as variables surface elevation $\bar{\eta}$ and horizontal momentum $\bar{q}$. In the porous domain, we implement the three-layer Boussinesq Eqs. (21) and (25) in physical variables; they read

$$\bar{\eta}_{\bar{t}} - \bar{A}\bar{\eta}_{\bar{x}\bar{x}\bar{t}} = K_1\left(\bar{\eta}_{\bar{x}}(\bar{B} + R_{31}\bar{\eta})\right)_{\bar{x}} \tag{34}$$

$$\bar{Q} - \bar{C}\bar{Q}_{\bar{x}\bar{x}} = -(\bar{B} + \bar{\eta})\bar{\eta}_{\bar{x}}, \tag{35}$$

with physical parameters $\bar{A} \equiv \bar{h}_3^2 A$, $\bar{B} \equiv \bar{h}_3 B$, $\bar{C} \equiv \bar{h}_3^2 C$. We simulate a solitary wave initially located upstream of the emerged porous medium. As time progresses, the wave propagates through the porous medium and further generates reflected and transmitted waves. Here we show that the numerical predictor–corrector method as explained in Sect. 4 follows through and can be used for solitary wave simulation.

The predictor–corrector method for Boussinesq equations in free areas (32, 33) is described below. We first rewrite Eq. (33) as

$$\psi_{\bar{t}} = -\frac{1}{\bar{h}_3}\bar{q}\bar{q}_{\bar{x}} - gh_3\bar{\eta}_{\bar{x}}, \quad \text{with} \quad \psi = \bar{q} - \frac{1}{3}\bar{h}_3^2\bar{q}_{\bar{x}\bar{x}}. \tag{36}$$

The new variable ψ introduced here is just for computational needs. Its values at grid points relate to $\bar{q}$ values through a linear correspondence analogous to Eq. (30). The first step implements forward time forward space in Eqs. (32) and (36) for calculating predicted values, indicated by overlines, as follows:

$$\overline{\bar{\eta}_j^{n+1}} = \bar{\eta}_j^n - \frac{\Delta t}{\Delta x}\frac{1}{\bar{h}_3}\left\{(\bar{h}_3 + \bar{\eta}_j^n)(\bar{q}_{j+1}^n - \bar{q}_j^n) + \bar{q}_j^n(\bar{\eta}_{j+1}^n - \bar{\eta}_j^n)\right\}$$

$$\overline{\Psi_j^{n+1}} = \Psi_j^n + \frac{\Delta t}{\Delta x}\left\{-\frac{1}{\bar{h}_3}\bar{q}_j^n(\bar{q}_{j+1}^n - \bar{q}_j^n) - gh_3\left(\bar{\eta}_{j+1}^n - \bar{\eta}_j^n\right)\right\}.$$

The correction step is then

$$\bar{\eta}_j^{n+1} = \bar{\eta}_j^n$$
$$- \frac{\Delta t}{2\bar{h}_3}\left\{(\bar{h}_3 + \bar{\eta})\bar{q}_{\bar{x}}|_j^n + \bar{q}\bar{\eta}_{\bar{x}}|_j^n + \overline{(\bar{h}_3 + \bar{\eta})\bar{q}_{\bar{x}}|_j^{n+1}} + \overline{\bar{q}\bar{\eta}_{\bar{x}}|_j^{n+1}}\right\}$$

$$\Psi_j^{n+1} = \Psi_j^n$$
$$- \frac{\Delta t}{2}\left\{\frac{1}{\bar{h}_3}\bar{q}\bar{q}_{\bar{x}}|_j^n + gh_3\bar{\eta}_{\bar{x}}|_j^n + \frac{1}{\bar{h}_3}\overline{\bar{q}\bar{q}_{\bar{x}}|_j^{n+1}} + gh_3\overline{\bar{\eta}_{\bar{x}}|_j^{n+1}}\right\},$$

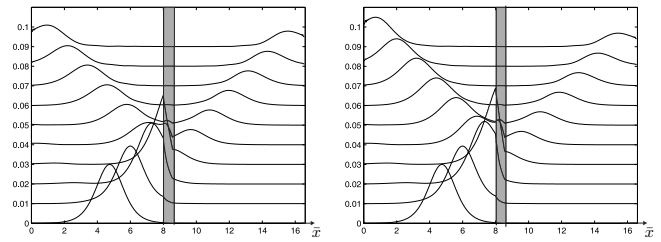**Fig. 5.** Surface elevation $\bar{\eta}(\bar{x}, \bar{t})$ at subsequent times $t_0 = 0 < t_1 < \ldots < t_{10} = 7\,\mathrm{s}$. Every following curve is shifted upwards to give a 3-dimensional impression. Left: $K_1 = 0.95$, $K_2 = 1$, $K_3 = 0.95\,\mathrm{cm\,s^{-1}}$, right: $K_1 = 0.7$, $K_2 = 0.75$, $K_3 = 0.7\,\mathrm{cm\,s^{-1}}$. All three layers are of the same thicknesses.

Table 2. Wave transmission coefficient for several lengths of porous medium, calculated using conductivity $K_1 = 0.7$, $K_2 = 0.75$ and $K_3 = 0.7\,\mathrm{cm\,s^{-1}}$ for $a/\bar{h}_3 = 0.1 - 0.4$.

Length L of porous belt				
20 cm	30 cm	40 cm	50 cm	60 cm
0.45–0.50	0.40–0.45	0.27–0.33	0.22–0.28	0.20–0.26

where we use forward space to compute $\bar{q}_{\bar{x}}|_j^n$, $\bar{\eta}_{\bar{x}}|_j^n$ and backward space to compute $\overline{\bar{q}_{\bar{x}}|_j^{n+1}}$, $\overline{\bar{\eta}_{\bar{x}}|_j^{n+1}}$.

Consider a computational domain with a porous domain in the middle, located on $[0, L]$. The approximate Eqs. (32) and (33), and the approximate of three-layer model Eqs. (21),(25) are combined. Vertical matching conditions come from the continuity of surface elevation

$$\bar{\eta}|_- = \bar{\eta}|_+, \tag{37}$$

where $-$ and $+$ denote the left-hand side and the right-hand side of the interface, respectively. In physical variables continuity of horizontal momentum is as follows:

$$\bar{q}|_{0^-} = K_1\bar{Q}|_{0^+}, \quad \bar{q}|_{L^+} = K_1\bar{Q}|_{L^-}, \tag{38}$$

where the term $K_1\bar{Q}$ denotes the reduced horizontal momentum in porous media. These matching conditions are commonly used for simulations of wave structure interaction, such as in Liu and Wen (1997), Lynett et.al. (2000), Scarlatos and Singh (1987), and Wang and Li (2002).

Here we show how the solitary wave evolves when it passes an emerged porous medium. The initial solitary wave profile of Boussinesq with amplitude a is as follows:

$$\bar{\eta}(\bar{x}, 0) = a\,\mathrm{sech}^2\left(\frac{3a}{4\bar{h}_3^3}\right)^{1/2}(\bar{x} - \bar{x}_0), \tag{39}$$

$$\bar{q}(\bar{x}, 0) = \frac{g\bar{h}_3^{3/2}}{\bar{h}_3 + \bar{\eta}(\bar{x}, 0)}\bar{\eta}(\bar{x}, 0), \tag{40}$$

which travels undisturbed in shape in free-water regions. Figure 5 presents simulation of an incoming solitary wave with

amplitude $a = 3$ cm on a water depth $\bar{h}_3 = 30$ cm passing through a porous medium (indicated in grey) with length $L = 60$ cm. As the soliton passes through the porous medium, reflected and transmitted waves occur. Amplitude ratio between these two waves depends on the precise detail of the emerged porous medium, i.e. its length L and its hydraulic conductivity K_i, $i = 1, 2, 3$. Smaller conductivity yields smaller amplitude of transmitted wave. For fixed conductivities, wave transmission coefficients are calculated for several lengths of porous medium, and the results are given in Table 2.

7 Conclusions

A non-linear, diffusive and dispersive Boussinesq equation has been derived for surface wave propagation in three-layer porous media. The equation reduces to the Boussinesq equation for one-layer porous media recorded in the literature. The predictor–corrector MacCormack method is a conditionally stable method for solving the three-layer Boussinesq equations. Numerical simulations of waves propagating into a three-layer system behave like waves propagating into a one-layer system, including the nonlinear effect: the rising of water level at the right end of porous breakwater. The engineering aspect of mangrove in reducing wave energy was considered here from the wave transmission coefficient curve, calculated for a porous belt with typical hydraulic conductivity of mangrove. Further, the MacCormack method was shown to be a stable numerical method for Boussinesq solitary waves. Simulation of reflected and transmitted waves as a result of an initial soliton passing through a three-layer porous medium was performed.

Appendix A

Appendix

Here we give a step-by-step derivation of the Boussinesq Eq. (21) from the full governing equations using the asymptotic expansion method. We start by solving the normalized Eqs. (13)–(20) layer by layer. Expand each potential Φ_i as a series in μ^2:

$$\Phi_i(x, z, t) = \Phi_{i0} + \mu^2 \Phi_{i1} + \mu^4 \Phi_{i2} + \cdots \quad \text{for} \quad i = 1, 2, 3. \quad \text{(A1)}$$

The first-order term Φ_{10} is a solution of the order-one term of the Laplace Eq. (13) with boundary condition (14); it reads $\Phi_{10}(x, z, t) = \eta(x, t)$. The first-order terms of interface condition (19) yield $\Phi_{i0}(x, z, t) = \eta(x, t)$ for $i = 2, 3$. Further, we consider terms of $\mathcal{O}(\mu^2)$ in equations for the upper-layer (13)–(15); those are

$$\Phi_{11zz} + \Phi_{10xx} = 0 \quad \text{in} \quad \Omega_1 \quad \text{(A2)}$$

$$\left(\eta_t - \varepsilon \eta_x^2\right) + \Phi_{11z} = 0 \quad \text{on} \quad z = \varepsilon \eta \quad \text{(A3)}$$

$$\Phi_{11} = 0 \quad \text{on} \quad z = \varepsilon \eta. \quad \text{(A4)}$$

Solving Eq. (A2) with $\Phi_{10} = \eta$ and using the boundary conditions (A3) and (A4) yields

$$\Phi_{11} = -\frac{1}{2}\eta_{xx}(z - \varepsilon \eta)^2 + \left(\varepsilon \eta_x^2 - \eta_t\right)(z - \varepsilon \eta). \quad \text{(A5)}$$

Next, the order $\mathcal{O}(\mu^2)$ of (16) is

$$\Phi_{21zz} + \Phi_{20xx} = 0 \quad \text{in} \quad \Omega_2. \quad \text{(A6)}$$

Solving the equation above with $\Phi_{20} = \eta$ and interface conditions (19) and (20) with Φ_{11} as given in Eq. (A5) yields

$$\begin{aligned}
\Phi_{21} = &-\frac{1}{2}\eta_{xx}\left\{(z + h_1)^2 + (h_1 + \varepsilon \eta)^2\right\} \\
&- \left(\varepsilon \eta_x^2 - \eta_t\right)(h_1 + \varepsilon \eta) \\
&+ R_{12}\left\{\eta_{xx}(h_1 + \varepsilon \eta) + \varepsilon \eta_x^2 - \eta_t\right\}(z + h_1),
\end{aligned} \quad \text{(A7)}$$

with $R_{ij} = K_i/K_j$ for $i, j = 1, 2, 3$. Next, the $\mathcal{O}(\mu^2)$ terms in equations for the third-layer (17) and (18) are

$$\Phi_{31zz} + \Phi_{30xx} = 0 \quad \text{in} \quad \Omega_3 \quad \text{(A8)}$$

$$\Phi_{31z} = 0 \quad \text{on} \quad z = -h_3 \quad \text{(A9)}$$

Solving Eq. (A8) with $\Phi_{30} = \eta$ and boundary condition (A9) and interface conditions (19) for $z = -h_2$ with Φ_{21} as in Eq. (A7) yields

$$\begin{aligned}
\Phi_{31} = &-\frac{1}{2}\eta_{xx}\left\{(z + h_3)^2 - (h_3 - h_2)^2 + (h_2 - h_1)^2 + (h_1 + \varepsilon \eta)^2\right\} \\
&+ R_{12}\left\{\eta_{xx}(h_1 + \varepsilon \eta) + \varepsilon \eta_x^2 - \eta_t\right\}(h_1 - h_2) \\
&- \left(\varepsilon \eta_x^2 - \eta_t/K_1\right)(h_1 + \varepsilon \eta).
\end{aligned} \quad \text{(A10)}$$

To get an approximate evolution equation of the order $\mathcal{O}(\mu^2)$ from the interface condition along $z = -h_2$, we still need to calculate the order-one term of Φ_{22z} and Φ_{32z}. Higher-order calculation is made under the assumption $\varepsilon = \mu^2$, and followed by collecting the $\mathcal{O}(\mu^4)$ terms. The equations for the first layer are

$$\Phi_{12zz} + \Phi_{11xx} = 0 \quad \text{in} \quad \Omega_1 \quad \text{(A11)}$$

$$-\Phi_{10x}\eta_x + \Phi_{12z} = 0 \quad \text{on} \quad z = \varepsilon \eta. \quad \text{(A12)}$$

Solving Eq. (A11) with the boundary conditions (A12) yields

$$\begin{aligned}
\Phi_{12z} = &\frac{1}{6}\eta_{4x}(z - \varepsilon \eta)^3 + \frac{1}{2K_1}\eta_{txx}(z - \varepsilon \eta)^2 \\
&+ \eta_x^2 + \mathcal{O}(\mu^2).
\end{aligned} \quad \text{(A13)}$$

Next, Φ_{22z} can be obtained from the $\mathcal{O}(\mu^4)$ term in the equation for the second layer

$$\Phi_{22zz} + \Phi_{21xx} = 0 \quad \text{in} \quad \Omega_2 \quad \text{(A14)}$$

with the boundary condition (20) for $z = -h_1$, and we get

$$
\begin{aligned}
\Phi_{22z} = {} & \frac{1}{6}\eta_{4x}(z+h_1)^3 + \left\{\frac{1}{2}\eta_{4x}h_1^2 - h_1\eta_{txx}\right\}(z+h_1) \\
& - R_{12}\left\{\eta_{4x}h_1 - \eta_{txx}\right\}\frac{1}{2}(z+h_1)^2 \\
& + R_{12}\left\{-\frac{1}{6}\eta_{4x}h_1^3 + \frac{1}{2}h_1^2\eta_{txx} + \eta_x^2\right\} + \mathcal{O}(\mu^2). \quad \text{(A15)}
\end{aligned}
$$

Next, collecting the $\mathcal{O}(\mu^4)$ terms in the equations for the third layer, we get

$$
\Phi_{32zz} + \Phi_{31xx} = 0 \quad \text{in} \quad \Omega_3 \tag{A16}
$$

$$
\Phi_{32z} = 0 \quad \text{on} \quad z = -h_3. \tag{A17}
$$

Solving Eq. (A16) with boundary conditions (A17) yields

$$
\begin{aligned}
\Phi_{32z} = {} & \frac{1}{6}\eta_{4x}(z+h_3)^3 \\
& + \frac{1}{2}\eta_{4x}\left\{-(h_3-h_2)^2 + (h_2-h_1)^2 + h_1^2\right\}(z+h_3) \\
& - \left\{R_{12}(\eta_{4x}h_1 - \eta_{txx})(h_1-h_2) + h_1\eta_{txx}\right\}(z+h_3) \\
& + \mathcal{O}(\mu^2). \tag{A18}
\end{aligned}
$$

Substituting Eqs. (A7), (A10) and (A15), (A18) into the interface condition (20) along $z = -h_2$ yields the following equation:

$$
\eta_t - \mu^2 A\eta_{xxt} = (\eta_x(B + \varepsilon R_{31}\eta))_x, \tag{A19}
$$

with A and B given in Eqs. (23) and (22), respectively. Hence, the approximate Boussinesq Eq. (A19) has been derived.

Edited by: R. Grimshaw
Reviewed by: S. N. Bora, N. Fowkes, and one anonymous referee

References

Chwang, A. T. and Chan, A. T.: Interaction between porous media and wave motion, Annu. Rev. Fluid Mech., 30, 53–84, 1998.

Dahdouh-Guebas, F.: Mangrove forests and tsunami protection, 2006 McGraw-Hill Yearbook of Science & Technology, McGraw-Hill Professional, New York, USA, 187–191, 2006.

Fernando, H. J. S., Samarawickrama, S. P., Balasubramanian, S., Hettiarachchi, S. S. L., and Voropayev, S.: Effects of porous barriers such as coral reefs on coastal wave propagation, Journal of Hydro-environment Research, 1, 187–194, 2008.

Kathiresan, K. and Rajendran, N.: Comments on "Coastal mangrove forests mitigated tsunami", Estuar Coast. Shelf S., 67, 539–541, 2006.

Lynett, P. J., Liu, P. L. F., Losada, I. J., and Vidal, C.: Solitary wave interaction with porous breakwaters, J. Waterw. Port C.-ASCE, 314–322, 2000.

Madsen, O. S.: Wave transmission through porous structures, J. Waterway Div.-ASCE, 100, 169–188, 1974.

Masda, Y., Magi, M., Kogo, M., and Nguyen Hong, P.: Mangrove as a coastal protection from waves in the Tong King delta, Vietnam, Mangroves and Salt Marshes, 1, 127–135, 1997.

Massel, S. R., Furukawa, K., and Brinkman, R. M.: Surface wave propagation in mangrove forests, Fluid Dyn. Res., 24, 219–249, 1999.

Nielsen, P.: Tidal dynamics of the water table in beaches, Water Resour. Res., 26, 2127–2134, 1990.

Lin, P. and Anuja Karunarathna, S. A. S.: Numerical Study of Solitary Wave Interaction with Porous Breakwaters, J Waterw. Port C.-ASCE, 133, 352–363, doi:10.1061/(ASCE)0733-950X(2007)133:5(352), 2007.

Liu, P. L. F. and Jiangang Wen, J.: Nonlinear diffusive surface waves in porous media, J. Fluid Mech., 347, 119–139, 1997.

Liu, P. L. F., Lin, P., Chang, K. A., and Sakakiyama, T.: Numerical modeling of wave interaction with porous structures, J. Waterw. Port C.-ASCE, 125, 322–330, doi:10.1061/(ASCE)0733-950X(1999)125:6(322), 1999.

Liu, W. C., Hsu, M.H., and Wang, C.F.: Modeling of Flow Resistance in Mangrove Swamp at Mouth of Tidal Keelung River, Taiwan, J. Waterw. Port C.-ASCE, 129, 86–92, doi:10.1061/(ASCE)0733-950X(2003)129:2(86), 2003.

Scarlatos, P. D. and Singh, V. P.: Long wave transmission through porous breakwaters, Coast. Eng., 11, 141–157, 1987.

Sollitt, C. K. and Cross, R. H.: Long-wave transmission through porous breakwaters, in: Proc. 13th Coastal Eng. Conf., ASCE, New York, USA, 3, 1827–1846, 1972.

Sulisz, W.: Wave reflection and transmission at permeable breakwaters of arbitrary cross-section, Coast. Eng., 9, 371–386, 1985.

Susilo, A. and Ridd, P. V.: The bulk hydraulic conductivity of mangrove soil perforated with animal burrows, Wetl. Ecol. Manag., 13, 123–133, 2005.

Teh, S. Y., Koh, H. L., Liu, P. L. F., Ismail, A. I. Md., and Lee, H. L.: Analytical and numerical simulation of tsunami mitigation by mangroves in Penang, Malaysia, J. Asian Earth Sci., 36, 38–46, 2009.

van Gent, M. R. A.: Wave interaction with permeable coastal structure, Ph.D. thesis, Delft University, Delft, the Netherlands, 1995.

Vo-Luong, H. P. and Massel, S.: Energy dissipation in non-uniform mangrove forests of arbitrary depth, J. Marine Syst., 74, 603–662, 2008.

Wang, K. H. and Li, W.: Modeling propagation of nonlinear shallow-water waves past a porous barrier, in: Proc. 15th Eng. Mech. Div. Conf. of the American Soc. of Civil Engineers, Columbia University, New York, USA, 2–5 June 2002.

Whitham, G. B.: Linear and Nonlinear Waves, John Wiley & Sons, Inc., New York, USA, 1973.